2007 IEEE International Conference on
Robotics and Automation
Roma, Italy, 10-14 April 2007

Control of a Snake-like Robot Using the Screw Drive Mechanism

Masaya Hara, Shogo Satomura, Hiroaki Fukushima, Tetsushi Kamegawa, Hiroki Igarashi and Fumitoshi Matsuno

Abstract— **In this paper, we develop a prototype of a new snake-like robot using the screw drive mechanism, and design a control system design for trajectory tracking. First, we explain the outline of the snake-like robot using the screw drive units and joint units, as well as the principle of the screw drive mechanism. Next, in order to achieve the trajectory tracking of the robot, we derive a kinematic model. Finally, the validity of the derived model and the effectiveness of the proposed control system are demonstrated by simulations and experiments.**

I. INTRODUCTION

The development of mobile robots for search and rescue operations in hazardous environments has been an active research area in recent years. One promising type of rescue robots is the so called snake-like robot, which is typically composed of three or more segments connected serially. Because of the long and slender shape, snake-like robots are expected to be effective for searches in narrow spaces and over rubbles in quake-devastated regions, etc [1][2][3]. Also, snake-like robots for pipe inspection have been reported in the literature [4][5]. A typical way of locomotion for snake-like robots is the one by undulations, which imitates real snakes' movements [2][3]. However, this type of locomotion needs a width for undulations.

On the other hand, snake-like robots driven by crawler mechanisms have been developed [1][6]. One limitation of typical crawler-type robots arises in vertically narrow spaces, where the upper part of the robots could hit the ceiling. In those cases, the robots could be stuck easily, since the upper and lower parts of the crawler drive the robot in opposite directions. To overcome this limitation, recent studies have proposed snake-like robots having crawlers on both upper and lower sides of the body [7][8].

Other types of locomotion mechanisms are found for pipe inspection robots in [4] and [5]. These robots need to press the body onto the inner wall to move in pipes, which limits to some extent the applicable size and shape of environments. Therefore, they are not necessarily suitable for rescue operations in various terrains.

Independently from these works, another snake-like robot using screw drive units connected serially has been proposed by the authors [9]. This robot can go into spaces as narrow as the width of the body, since undulations are not necessary. Also, it is expected that this robot does not get stuck easily even if the upper part of the body hit the ceiling, since the upper part of the screw unit drive the body in the same direction as the lower part. Furthermore, it can move in any direction unlike most existing snake-like robots. However, only the case, where the shape of the robot is fixed, has been considered. Therefore, it has not been clarified how this robot moves when both the screw drive units and the joints are actuated. For search operations in complex terrains, the robot needs to adopt its shape to the terrains by actuating the joints.

M. Hara, S. Satomura, H. Fukushima, and F. Matsuno are with the Department of Mechanical Engineering and Intelligent Systems, The University of Electro-Communications, Tokyo, Japan

T. Kamegawa is with the Department of Natural Science and Technology, Okayama University, Okayama, Japan

H. Igarashi is with SGI Japan, Tokyo, Japan

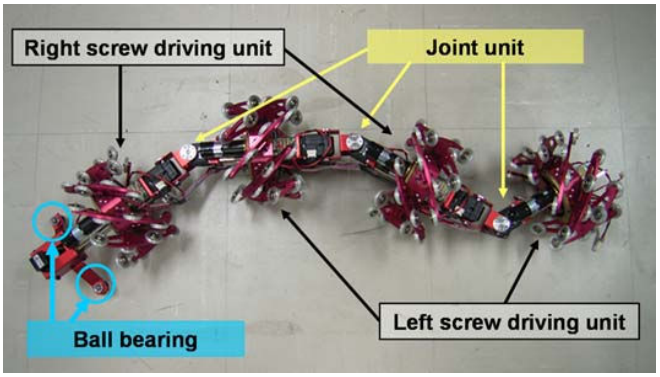

Fig. 1. Snake-like robot with screw drive units

In this paper, we develop a new prototype of the snake-like robot using screw-drive units connected by 2-degree-of-freedom (DOF) joints. Also, in order to achieve the trajectory tracking, we derive a kinematic model in the case where both the screw-drive units and the joints are actuated. Furthermore, the validity of the model and the effectiveness of the feedback control are demonstrated by simulations and experiments.

II. SNAKE-LIKE ROBOT WITH SCREW DRIVE MECHANISM

A. Snake-like robot with screw drive mechanism

Fig.1 shows the prototype of the snake-like robot using the screw drive mechanism, developed in this paper. The robot is comprised of two types of screw drive units, i.e. "left" and "right" screw units. In Fig.1, right and left units are connected alternatively from the top. The screw drive units are connected by 2-DOF active joints. Moreover, a caster with ball bearings is set up at the head of the robot to prevent the body inside the unit from rotating instead of the screws, when the shape of the robot is straight.

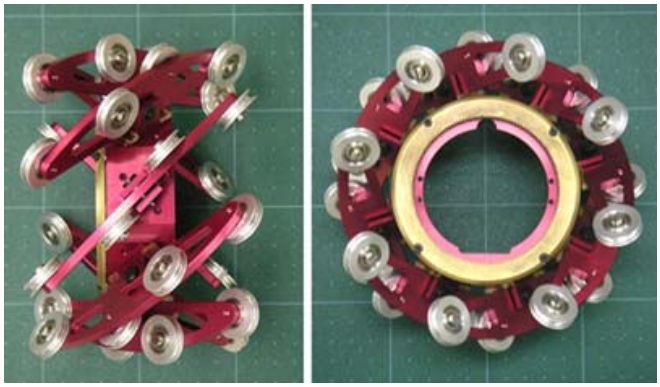

Fig. 2. Side and front view of screw drive unit

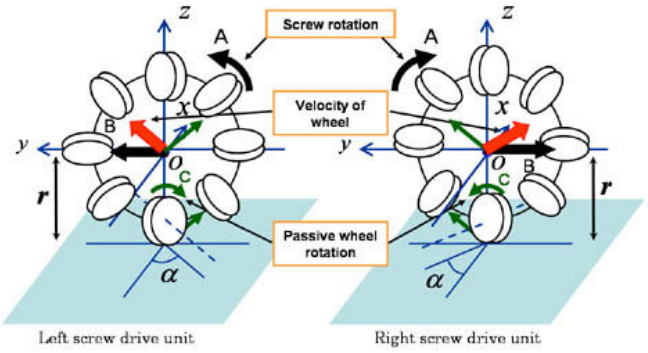

Fig. 4. Model of left and right screw drive units

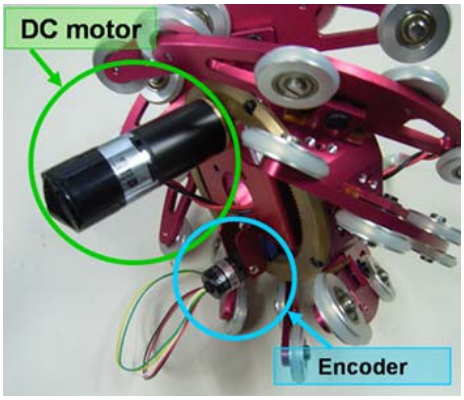

Fig. 3. Screw drive unit

Fig. 5. Joint unit

B. Screw drive unit

Fig.2 and Fig.3 show a screw drive unit. The screw unit is composed of the screw part, which actually rotates, and the body part which is equipped with a DC motor to drive the screw part. The screw part is comprised of eight braids along the outer circle, and four passive wheels are equipped with each braid. The angle between the rotation axes of the screw part and the passive wheel on the ground defined as α, as shown in Fig.4. In the case of positive (negative) α, the unit is defined a left (right) screw drive unit. Let the center of the screw drive unit be o, and $o - xyz$ is a coordinate system fixed to o.

When the screw drive unit rotates in the direction of the arrow A, translational velocity is caused to the center point o in the direction of the arrow B. At the same time, the passive wheel rotates in the direction of the arrow C. Therefore, the velocity of the screw drive unit is consequently generated in the direction of the rotation axis of the passive wheel on the ground (the same direction as the arrow from the center point o). Here, r denotes the radius of the screw drive unit (distance from the center of the unit to the ground).

C. Joint unit

Fig.5 shows a joint unit. Two actuators are equipped for pitch and yaw angles. Each actuator has a 90-degree range of movement. The rotation angle and angular velocity of the motor can be measured and controlled with a resolution 1024 per rotation.

D. Electrical system of the snake-like robot using the screw drive mechanism

Fig.6 shows the control system of the snake-like robot using the screw drive mechanism. The electrical system is divided into two main parts, the screw drive unit part and the joint unit part. The screw drive unit part, communicates with a personal computer (PC) by using RS485, and the joint unit part communicates with the PC by using RS232C.

Furthermore, one host microcomputer is equipped on the tail of the robot for a relay between the unit and the PC. Each screw drive unit equips a microcomputer, a motor driver for the DC motor (Maxon, A-max22), and an encoder to control angular velocity.

For velocity control of the motor of the screw unit, first, a target value of angular velocity is sent from the PC to the microcomputer. Next, the Pulse Width Modulation (PWM) signal is given from the microcomputer to the motor driver to drive the DC motor. The count value of the encoder is obtained by the microcomputer as information on the rotation angle of the screw part. The microcomputer communicates each other by using Controller Area Network (CAN).

The motors for the joint units (BestTechnology, Dynamixel DX-117) can be connected in a daisy chain, and the motor in the end is connected to the PC for control by using RS485.

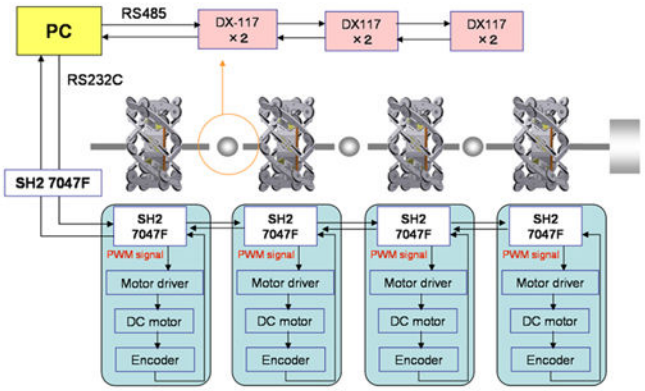

Fig. 6. Architecture of the robot

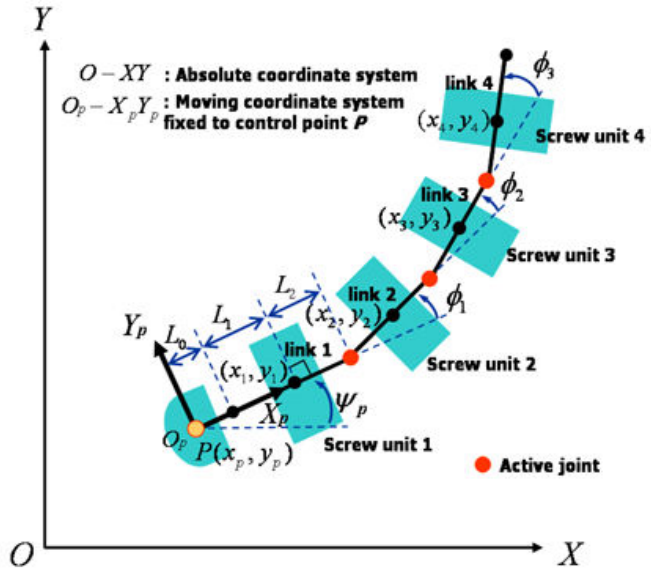

Fig. 7. Model of a screw drive snake-like robot

III. CONTROL SYSTEM DESIGN BASED ON MODEL

A. Derivation of kinematic model

In this section, we derive a kinematic model comprised of 4 screw drive units described in Section II. The passive wheels attached on the screw drive unit is assumed not to slip in this paper.

As shown in Fig.7, let the point O be the origin of the absolute coordinate system, P be the point to be controlled, $O-XY$ be the absolute coordinate system, $O_p-X_pY_p$ be the local coordinate system fixed to P. Also, let $[x_p\ y_p\ \psi_p]^T$ be the position of P and the orientation of the local coordinate system $O_p - X_pY_p$ with respect to the absolute coordinate system, $[x_i\ y_i]^T$ be the position of the center of the screw unit i with respect to the absolute coordinate system. Furthermore, let L_0 be the length from control point P to the tip of link 1, L_1 be the length from the tip of each link to the center of the screw drive unit on the link, L_2 be the length from the center of the screw unit to the terminal of the link. Let α_i be the angle between the rotational axes of the i-th screw drive unit and the passive wheel, ϕ_i be the orientation of the link i with respect to the link $i+1$, and $\psi_i = \psi_p + \sum_{k=1}^{i-1} \phi_k (i = 2, 3, 4)$ be the orientation of the link i with respect to the absolute coordinate system. Additionally, let $\dot{\theta}_i (i = 1, 2, 3, 4)$ be the angular velocity of the screw drive unit i.

The position of the center of the screw unit i is described from a geometrical relation as follows:

$$x_i = x_p + (L_0 + L_1)\cos\psi_p + \sum_{j=1}^{i-1}(L_2\cos\psi_j + L_1\cos\psi_{j+1}), \tag{1}$$

$$y_i = y_p + (L_0 + L_1)\sin\psi_p + \sum_{j=1}^{i-1}(L_2\sin\psi_j + L_1\sin\psi_{j+1}). \tag{2}$$

Since it is assumed that the passive wheels do not slip sideways, we need to take into account the velocity constraint condition. The velocity constraint condition here is more complicated than conventional snake-like robots [9][10] because of the screw units. The white rectangular in Fig.8 shows the passive wheel, which contacts with the ground, of the ith screw unit (black rectangular). If the screw drive unit i rotates at angular velocity $\dot{\theta}_i$, the velocity $r\dot{\theta}_i$ is caused for the passive wheel. The velocity component in the direction of the axle of the passive is becomes $r\dot{\theta}_i \sin\alpha_i$. The $X-$ and $Y-$components $\dot{x}_i$ and $\dot{y}_i$ of the velocity of the unit i cause the velocities $\dot{x}_i\cos(\alpha_i + \psi_i)$ and $\dot{y}_i\sin(\alpha_i + \psi_i)$ in the direction of the axle of the passive wheel. Therefore, the velocity constraint condition is described as follows:

$$\dot{x}_i\cos(\alpha_i + \psi_i) + \dot{y}_i\sin(\alpha_i + \psi_i) + r\dot{\theta}_i\sin\alpha_i = 0. \tag{3}$$

By substituting the derivatives of (1)−(2) into (3), the following kinematic model is obtained:

$$A(w)\dot{w} = B(w)u, \tag{4}$$

where, $w = [x_p\ y_p\ \psi_p\ \phi_1\ \phi_2\ \phi_3]^T$ is the state vector to be controlled, $u = [\dot{\theta}_1\ \dot{\theta}_2\ \dot{\theta}_3\ \dot{\theta}_4\ \dot{\phi}_1\ \dot{\phi}_2\ \dot{\phi}_3]^T$ is the control input vector. Also, A and B are defined as follows:

$$A = \begin{bmatrix} a_{11} & a_{12} & a_{13} & 0 & 0 & 0 \\ a_{21} & a_{22} & a_{23} & a_{24} & 0 & 0 \\ a_{31} & a_{32} & a_{33} & a_{34} & a_{35} & 0 \\ a_{41} & a_{42} & a_{43} & a_{44} & a_{45} & a_{46} \\ 0 & 0 & 0 & 1 & 0 & 0 \\ 0 & 0 & 0 & 0 & 1 & 0 \\ 0 & 0 & 0 & 0 & 0 & 1 \end{bmatrix}, \tag{5}$$

$$B = \text{block diag}(-r\sin\alpha_i E_4, E_3), \tag{6}$$

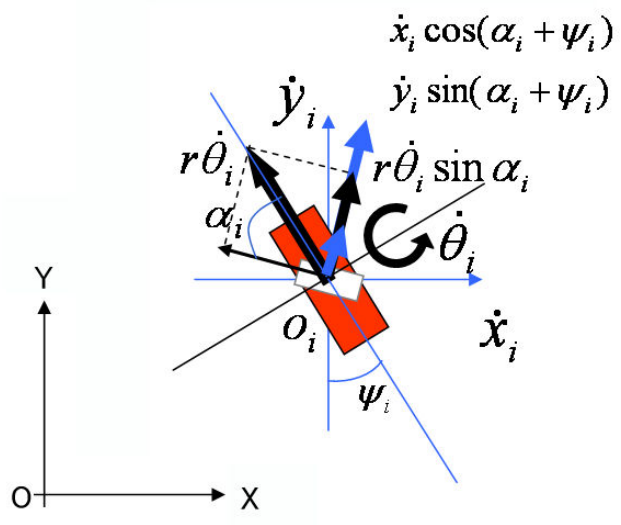

Fig. 8. Velocity constraint for a passive wheel of the screw unit i

$$
\begin{aligned}
a_{i1} &= \cos(\alpha_i+\psi_i)\\
a_{i2} &= \sin(\alpha_i+\psi_i)\\
a_{13} &= (L_0+L_1)\sin\alpha_1\\
a_{23} &= L\sin(\alpha_2+\phi_1)+L_1\sin\alpha_2\\
a_{24} &= L_1\sin\alpha_2\\
a_{33} &= L\sin(\alpha_3+\phi_1+\phi_2)+a_{34}\\
a_{34} &= (L_1+L_2)\sin(\alpha_3+\phi_2)+L_1\sin\alpha_3\\
a_{35} &= L_1\sin\alpha_3\\
a_{43} &= L\sin(\alpha_4+\phi_1+\phi_2+\phi_3)+a_{44}\\
a_{44} &= (L_1+L_2)\sin(\alpha_4+\phi_2+\phi_3)+a_{45}\\
a_{45} &= (L_1+L_2)\sin(\alpha_4+\phi_3)+L_1\sin\alpha_4\\
a_{46} &= L_1\sin\alpha_4,
\end{aligned}
$$

where $L:=L_0+L_1+L_2$, and E_k is the identity matrix of size k.

B. Trajectory control law

For the system in (4), the control input for trajectory tracking is designed as follows:

$$u = B^{-1}A(\dot{w}_d - Ke), \tag{7}$$

where $e=w-w_d$, w_d is the given target trajectory, and K is a given feedback gain matrix. By substituting (7) into (4), the closed-loop system is given as

$$A(\dot{e}+Ke)=0. \tag{8}$$

If the matrix A is full column rank, then it holds $\dot{e}+Ke=0$. Therefore $w\to w_d(t\to\infty)$ is guaranteed if k is positive definite.

IV. SIMULATION

In this section, the effectiveness of the model and the control law described in section III is demonstrated by simulations. Each parameter in the simulations is decided as follows, based on the prototype in section II.

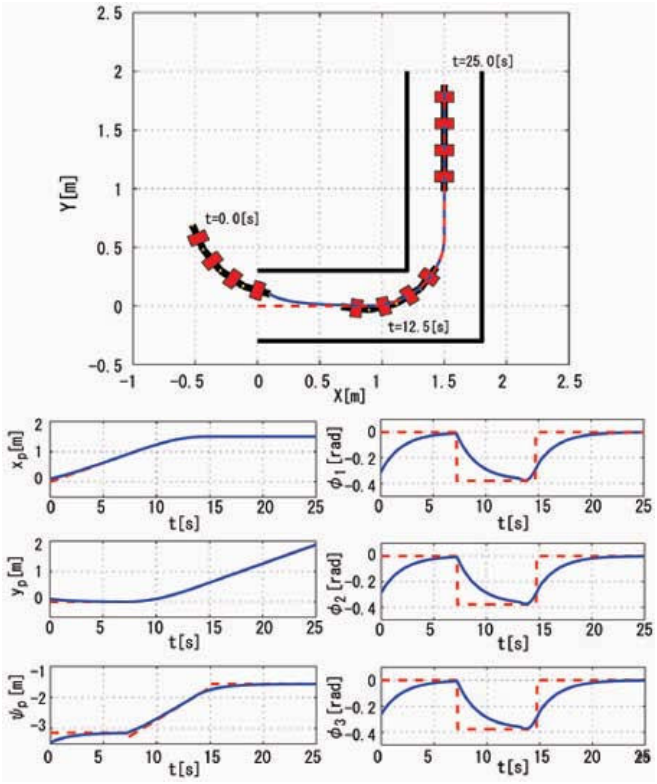

Fig. 9. Simulation result for the L-type crank path

$$
\begin{aligned}
\alpha_i &= -\frac{\pi}{4}[\mathrm{rad}](i=1,3), \quad \alpha_i=\frac{\pi}{4}[\mathrm{rad}](i=2,4),\\
r &= 0.075[\mathrm{m}], \quad L_0=0[\mathrm{m}],\\
L_1 &= 0.103[\mathrm{m}], \quad L_2=0.123[\mathrm{m}].
\end{aligned}
$$

We consider the trajectory in the corner as shown in Fig.9. We set the $w(0)=[0.1,0.1,-\frac{11\pi}{10},-\frac{\pi}{10},-\frac{\pi}{11},-\frac{\pi}{12}]^T$, $v=0.125$[m/s] as translational velocity of the target position, and $K=\frac{1}{2}E_6$. In the corner, we give the target joint angles, such that the robot changes the shape along the curve with radius 0.6[m]. The simulation time is 25[s], and the width of the route is 0.6[m].

The figure on the top shows the $X-Y$ plot of the trajectory of the point P on the robot, and the figures in the lower part indicate the time responses of the states. The broken lines in the figures indicate the desired values, and the solid lines show the responses of the states. From this result, it can be seen that the each state converges to the desired value, and the robot moves along the target trajectory. Furthermore, the result shows that the trajectory tracking is achieved even when the joint angles are changing.

V. EXPERIMENT

In this section, the effectiveness of the model and the control law described in Section III is demonstrated by experiments using the prototype in Section II. The position and the posture of the head $[x_p,y_p,\psi_p]^T$ are measured by

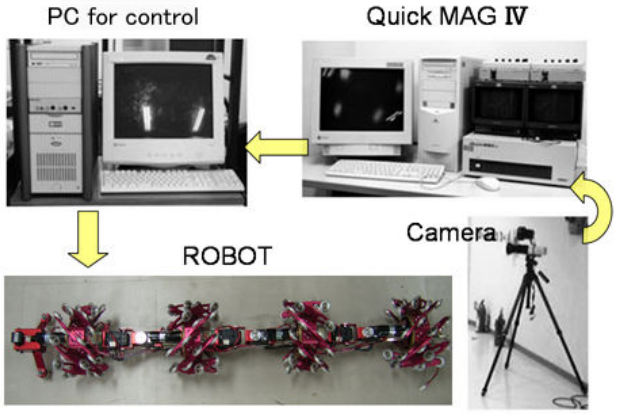

Fig. 10. Experimental system

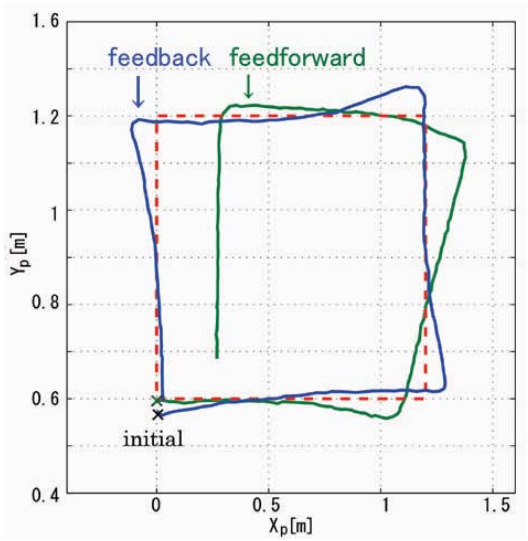

Fig. 11. Experimental results of the feedforward control and the feedback control for a square path

a 3D motion analysis system using 2 overhead cameras. The control input in (7) is computed by a PC using the measurement data of w.

We shows the results of two kinds of experiments. The first is the case where the each joint angle is fixed to the initial condition. The second is the case where the joint angles are changed while the robot is moving.

(i) The case of fixed joint angles

The feedforward control based on the model in (4) and the feedback control in (7) are applied for the square target trajectory (1.2×1.2[m]), as shown by the broken line in Fig.11 and Fig.12. The joint angles are fixed to $\phi_1 = \phi_2 = \phi_3 = 0$[rad]. The initial posture of the head is set to $\psi_p(0) = 0$ [rad]. Where, we set the translational velocity of the target position to 0.2[m/s] and the feedback gain to $K = diag(0.5, 0.5, 0.5, 0, 0, 0)$.

Fig.11 shows $X-Y$ plots of the trajectories of P for the feedforward control and the feedback control. Fig.12 shows the time responses of the position and the posture of P.

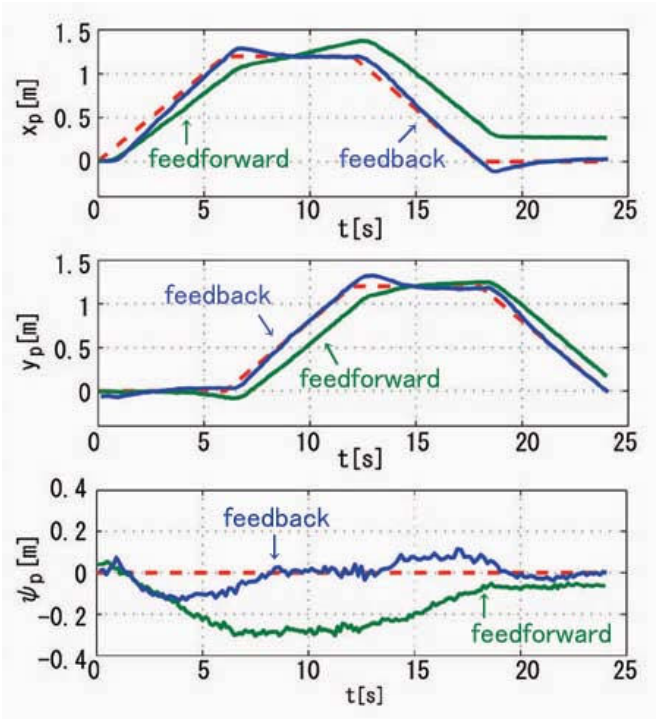

Fig. 12. Experimental results of the feedforward control and the feedback control for a square path

From the experimental result for feedforward control, it can be seen that the trajectory error of P is accumulated due to the large deviation of the posture ψ_p. On the other hand, the tracking performance is improved by feedback control.

(ii) The case of variable joint angles

The feedback control in (7) is applied for the same target trajectory as in Section IV. We set the initial state to $w(0) = [0.1, 0.04, -3.32, -\frac{\pi}{9}, -\frac{\pi}{10}, -\frac{\pi}{11}]^T$, the translational velocity to 0.125[m/s], and the feedback gain to $K = \frac{1}{2}E_6$.

Fig.13 shows the experimental result. The figure on the top shows the $X-Y$ plot of the trajectory of P and the figures in the lower part indicate the time response of the states. The broken lines indicate the desired values, and the solid lines indicate the responses of the states by feedback control. From this result, it can be seen that the each state converges to the desired value, and the robot moves along the target trajectory. Furthermore, the result shows that the trajectory tracking is achieved even when the joint angles are changing. On the other hand, the steady-state error which is not seen in the simulation, was caused for the each joint angle. Possible reasons are the friction with the ground, side slipping of the passive wheels, and the load due to the communications cables.

VI. CONCLUSIONS AND FUTURE WORKS

In this paper, we have derived a kinematic model of the snake-like robot using the screw drive mechanism connected by two-degree-of-freedom joints. Also, we have designed a control system based on the kinematic model. Moreover,

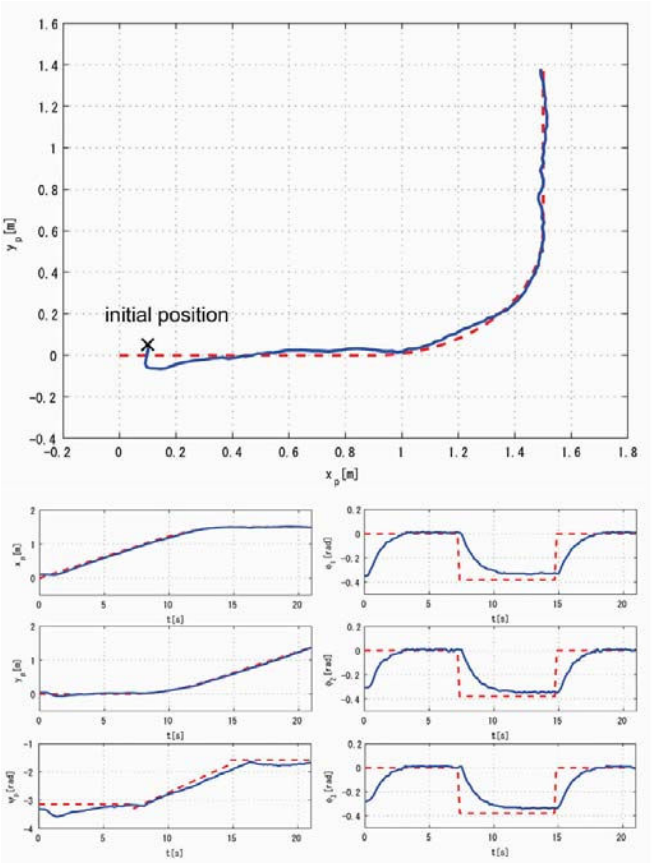

Fig. 13. Experimental result of feedback control for L-type crank path

through the trajectory tracking control simulations and experiments, effectiveness of the derived control law has been demonstrated.

Possible future works are three-dimensional motion analysis using more effectively the two-degree-of-freedom joints, and analysis when the number of units is increased to give the redundancy. Furthermore, force control based on a dynamic model is necessary to realize the tasks as climbing a tree.

ACKNOWLEDGMENTS

This research was supported in part by the Ministry of Education, Culture, Sports, Science and Technology Grant-in-Aid for Scientific Research (No.17360105).

REFERENCES

[1] Tetsushi Kamegawa, Tatsuhiro Yamasaki, Hiroki Igarashi, and Fumitoshi Matsuno• ”Development of The Snake-like Rescue Robot KOHGA” Proc. IEEE International Conference on Robotics and Automation 2004. (CD-ROM)

[2] T.Kamegawa and F.Matsuno: ”Proposition of Twisting Mode of Locomotion and GA Based Motion Planning for Transition of Locomotion Modes of 3-Dimensional Snake-Like Robot” Proceedings of the 2002 IEEE International Conference on Robotics and Automation, ICRA 2002, May 11-15, pp.1507-1512, 2002, Washington, DC, USA.

[3] M.Mori and S.Hirose• ”Development of Active Cord Mechanism ACM-R3 with Agile 3D mobility” Proc. IEEE/RSJ International Conf. on Intellegent Robots and Systems, pp.1552-1557,2001

[4] S.Hirose,H.Ohno,T.Mitsui,and K.Suyama• ”Design and Experiments of In-pipe Inspection Vehicles for $\phi 25, \phi 50, \phi 250$ Pipes” Journal of Robotics and Mechatronics, Vol. 12,No.3, pp.310-317, 2000

[5] Toshiaki Yamaguchi, Yoshihito Kagawa, Iwao Hayashi, Nobuyuki Iwatsuki, Kouichi Morikawa, K.atsumi Nakamura: ”Screw Principle Microrobot Passing Steps in a Small Pipe” Proc. of the 1999 International Symposium on Micromechatronics and Human Science, pp.149-152, 1999

[6] Toshio Takayama and Shigeo Hirose• ”Development of ”Souryu IÍ Ⅱ ” -Connected Crawler Vehicle for Inspection of Narrow and Winding Space-” Journal of Robotics and Mechatronics, Vol.15,No.1, pp.61-69, 2001

[7] K.Osuka and H.Kitajima: ”Development of Mobile Inspection Robot for Rescue Activities: MOIRA” Proc. of the IEEE/RSJ Int. Conference on Intelligent Robots and System, pp. 3373ᴹ 3377, 2003

[8] Johann Borenstein, Malik Hansen, and Hung Nguyen: ”The OmniTread OT-4 Serpentine Robot for Emergencies and Hazardous Environments” 2006 International Joint Topical Meeting: Sharing Solutions for Emergencies and Hazardous Environments, ¡ February 12-15, 2006, Salt Lake City, Utah, USA

[9] F.Matsuno, Y.Semba, T.Kawai, and M.Tanaka: ”Control of Robot with Screw Drive Mechanism” Trans. Society of Instrument and Control Engineers, submitted 2004, (in Japanese)

[10] F. Matsuno and K.Mogi: ”Redundancy Controllable System and Control of Snake Robots Based on Kinematic Model” Proceedings of the $39^{\mathbf{th}}$ IEEE Conference on Decision and Control Sydney, Australia December, 2000